ORIGINAL CONTRIBUTION

DODAB and DODAC bilayer-like aggregates in the micromolar surfactant concentration domain

Eloi Feitosa · Fernanda Rosa Alves ·
Elisabete M. S. Castanheira ·
M. Elisabete C. D. Real Oliveira

Abstract In the millimolar concentration domain (typically 1 mM), dioctadecyldimethylammonium bromide and chloride (DODAX, X representing Br^- or Cl^- counterions) molecules assemble in water as large unilamellar vesicles. Differential-scanning calorimetry (DSC) is a suitable technique to obtain the melting temperature (T_m) characteristic of surfactant bilayers, while fluorescence spectroscopy detects formation of surfactant aggregates, like bilayers. These two techniques were combined to investigate the assembly of DODAX molecules at micromolar concentrations, from 10 to 100 μM. At 1 mM surfactant, $T_m \approx 45\,°C$ and $49\,°C$, respectively, for DODAB and DODAC. DSC and fluorescence of Nile Red were used to show the formation of DODAX aggregates, at the surfactant concentration as low as 10 μM, whose T_m decreases monotonically with increasing DODAX concentration to attain the value for the ordinary vesicles. The data indicate that these aggregates are organized as bilayer-like structures.

E. Feitosa
Physics Department, São Paulo State University,
São José do Rio Preto, SP, Brazil

F. R. Alves · E. M. S. Castanheira
Instituto de Química, Universidade Estadual de Campinas,
Campinas, SP, Brazil

M. E. C. D. R. Oliveira
Physics Department, University of Minho,
Campus de Gualtar,
4710-057 Braga, Portugal

E. Feitosa (✉)
Physics Department, IBILCE/UNESP,
Rua Cristovao Colombo, 2265,
Sao Jose do Rio Preto, SP, Brazil CEP: 15054-000
e-mail: eloi@ibilce.unesp.br

Introduction

There is a class of surfactants suitable to form vesicles in aqueous solutions, that is, closed bilayers entrapping a limited portion of the aqueous solvent, the water core, where hydrophilic solutes can be solubilized [1]. These vesicles have potential applications in drug delivery as well as to mimic biomembranes [1, 2]. Other solubilization sites for small particles are the vesicle bilayer, where hydrophobic molecules can be solubilized, and the inner and outer vesicle interfaces where polar and amphiphilic molecules can be anchored.

It is well established that dioctadecyldimethylammonium bromide and chloride (DODAB and DODAC) molecules assemble as cationic vesicles with properties and structure that depend on the surfactant concentration, solvent condition (ionic strength and temperature) and method of vesicle preparation [3–11]. Large unilamellar vesicles (LUV) can be formed by simply warming an aqueous mixture of DODAX (typically 1 mM) to 55–60 °C (i.e., safely above the T_m of these surfactants). Multilamellar and multistructural vesicles can also be formed at higher surfactant concentrations, as well as in presence of single inorganic salts [9]. Thus, surfactant concentration, ionic strength, and temperature contribute to determine the vesicle structure in DODAX aqueous dispersions. Overall, the structure of the surfactant aggregates becomes more complex when the surfactant concentration is raised or temperature is lowered below T_m. DODAB or DODAC vesicle instability and polydispersity tend to increase with

the surfactant concentration, because at higher concentrations, the vesicles are closer together and the intervesicle interactions are destabilizing [7, 9, 11].

Stable (or meta-stable) unilamellar vesicles can thus be prepared within a quite limited range of surfactant concentrations. Higher DODAX concentrations favor the formation of more complex structures as well as vesicle fusion and precipitation [7, 9]. The opposite behavior is thus expected for very dilute dispersions. That is, dilute vesicles might be more stable and less polydisperse than the ordinary vesicles.

Long-chain vesicle-forming surfactants like DODAX exhibit a small critical vesicle concentration (CVC), above which, vesicles are formed. The CVC of DODAB or DODAC is too low to be measured by ordinary techniques (for instance surface tension, conductimetry, light-scattering, etc.) [5], and allows the formation of cationic aggregates in the domain of micromolar concentrations.

In this communication, highly sensitive differential-scanning calorimetry (DSC) and steady-state fluorescence of the probe Nile Red (NR) were used to detect DODAB and DODAC aggregates at surfactant concentrations as low as $10 \mu M$. The data are compared to those for ordinary millimolar vesicles. The DSC thermograms for the diluted dispersions exhibit a single endothermic peak characteristic of T_m for bilayers while the fluorescent data indicate the presence of hydrophobic regions surrounding the fluorescence probe. The effect of DODAX concentration on T_m allows a comprehension of some properties of the aggregates that may be highly suitable as host for microamount of solute molecules. The NR fluorescence spectra monitored at varying DODAX concentration also support the formation of surfactant aggregates. It is worth mentioning that at such low concentrations the samples are "invisible" to important techniques available to investigate bilayer structures, such as light-scattering, conductimetry, tensiometry, or cryo-TEM.

Materials and methods

DODAB (from Sigma) was recrystallized and DODAC was obtained from DODAB by ion exchange and recrystallized as reported [4]. Ordinary 1.0 mM DODAB and DODAC vesicles were prepared by mixing the surfactant and water at room temperature (ca 22 °C) and warming the mixture to 60 °C until complete dissolution of the surfactant. The homogeneous dispersions were then cooled to room temperature for storage. These vesicles can alternatively be stored at the fridge temperature (5 °C), where they are as well stable for months [9, 11]. The micromolar samples were obtained by diluting at room temperature (below T_m) the stock vesicle dispersions of DODAX, 1.0 mM, to the desired concentration of the surfactant for DSC and

fluorescence measurements. For comparison, ordinary 1.0 mM DODAX dispersions were also investigated by DSC and fluorescence, and a systematic investigation was performed for DODAX concentrations below 0.1 mM. Ultrapure Milli-Q-Plus quality water was used in sample preparations.

Differential-scanning calorimetry

DSC experiments were performed in a highly sensitive DSC model VP-DSC MicroCal MC-2 (MicroCal Inc., Northampton, MA, USA), equipped with 0.542 ml twin cells for the reference and sample solutions. Heat was supplied to or removed from the sample and reference and the equipment recorded the power removed from or supplied to the sample, to keep its temperature equal to the reference temperature, as the cell temperature was varied at a constant rate. The power was then converted to heat and the equipment supplied the heat capacity at constant pressure (ΔC_p) for the sample, as a function of temperature (thermogram). Associated to the melting transition (and other transitions), there is a peak in the DSC traces which maximum is positioned at T_m. The melting enthalpy is proportional to the peak area, that is, $\Delta H = \int C_p dT$; the width of the peak is inversely proportional to the transition cooperativity. The measurements were performed with the scan rate of 1 °C/min and temperature range of 5–85 °C. Details on the experimental procedures can be found elsewhere [7, 9].

Steady-state fluorescence

The fluorescence probe 9-(diethyl-amino)-5H-benzo[a]phenoxazin-5-one (Nile Red, NR) was used as supplied by Aldrich. Nile Red was introduced in the DODAX/water systems by evaporating the appropriate volume of a 1 mM stock solution of the probe in ethanol, under an argon stream. Then, the required amount of 1.0 mM DODAX dispersion in water was added and the system was heated to 60 °C under vigorous stirring. The solutions were then cooled to room temperature and left standing for several hours (ca 24 h) to stabilize. The final concentration of NR in the solutions is $0.5 \mu M$.

Fluorescence measurements were performed using a Fluorolog 3 spectrofluorimeter, equipped with a temperature controlled cuvette holder. Polarized emission spectra were recorded using Glan−Thompson polarizers. All spectra were corrected for the instrumental response of the system.

Fluorescence measurements were performed below and above the melting temperature of both surfactants, respectively, at 25 and 60 °C. The spectra at both temperatures were repeated in different days to check reproducibility. All measurements were reproducible. Emission of Nile Red in

pure water was obtained for comparison immediately after solution preparation.

Results

DODAB and DODAC molecules assemble in water as vesicles, whose structure is determined by the surfactant concentration, counterion nature and temperature. In general, the vesicle structure tends to be more complex at higher surfactant concentration and lower temperature; qualitatively the complexity of the bilayer structure is viewed by the sample turbidity. The counterion Br⁻ also gives more complex vesicles (more turbid) than Cl⁻ [11]. At 1.0 mM, DODAB and DODAC vesicles exhibit typical DSC thermograms, as shown in Fig. 1. These surfactants exhibit, respectively, three and one peaks, indicating that the structure of DODAB vesicles is more complex at this concentration.

The effect of diluting the 1.0 mM DODAB and DODAC vesicle dispersions on the DSC thermogram is shown in Fig. 2. Below 40 μM, DODAB DSC thermograms are single-peak, indicating that the DODAB aggregates structure are similar to those of the ordinary vesicles. The precise structures of these aggregates cannot be inferred from the presented data. The melting temperature, melting enthalpy and peak width obtained from the thermograms are summarized in Figs. 3 and 4, and also in Table 1. The pre-transition temperature for DODAB lies within ca 30–33 °C (Fig. 2), and up to 100 mM DODAB does not exhibits a clear post-transition.

The fluorescence spectra of NR incorporated in DODAB and DODAC vesicles are depicted in Figs. 5 and 6, respectively, at 25 and 60 °C, that is, below and above T_m.
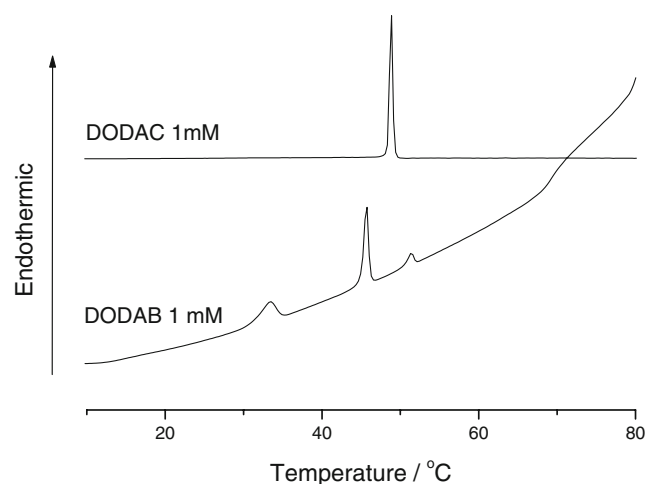

Fig. 1 Second DSC upscan thermograms for 1.0 mM DODAB and DODAC in aqueous dispersions, used as reference for the DSC data from micromolar samples

The NR spectral modifications due to change in surfactant concentration and temperature can give important information on the surfactant packing and bilayer structure. The effect of surfactant concentration on the variation of NR maximum emission wavelength, λ_{max}, and on the steady-state fluorescence anisotropy, is depicted in Figs. 7 and 8, respectively, at 25 and 60 °C. The results indicate that the probe feels two different environments with different levels of hydration. The fitting of the NR emission spectra to a sum of two lognormal functions is shown in Fig. 9 for 10 μM DODAC at 25 °C, as an example. The global fitting results for DODAB and DODAC are presented in Table 2.

Discussion

DSC results

DSC and fluorescence measurements for 1.0 mM DODAX dispersions were performed for comparison with the data in the micromolar concentration domain. Figure 1 compares the typical single- and three-peak DSC traces, respectively, for DODAC and DODAB. At 1.0 mM, DODAC vesicles in water exhibit a single-peak DSC thermogram due to the melting temperature at $T_m \approx 49.0$ °C, whereas DODAB vesicles exhibit two additional peaks to the main transition ($T_m \approx 45.8$ °C): the pre-transition ($T_s \approx 33.3$ °C) and the post-transition ($T_p \approx 51.5$ °C) peaks, in good agreement with previously reported data [7, 9]. Upon dilution, however, the DODAB post-transition peak disappears below 80 μM and the pre-transition one vanishes below 40 μM. According to Fig. 2, T_s lies between ca 30–33 °C for DODAB concentration in the range of 40–100 mM (Fig. 2). Thus, the single peak in the DSC thermograms below 40 μM DODAX aqueous dispersions is undoubtedly related to the main transition (chain melting) temperature, T_m, indicating that at quite low concentrations bilayer structures are formed.

Since the pre-transition is related to undulation in the vesicle bilayers [7], the absence of the pre-transition peak below 40 μM does not necessarily mean there is no undulation associated with the vesicle bilayer but, instead, the undulation energy may be too low to be detected by the calorimeter. The post-transition temperature may be related to the formation of local lamellar phases in the gel state (below T_m) yielding flow-birefringency, and the peak height tends to increase with surfactant concentration [7]. As below 80 μM, the aggregates exhibit no post-transition temperature, the dispersion may be dominated by bilayer structures and contains no local lamellar phases and the samples exhibit no flow-birefringency.

For both DODAB and DODAC, T_m increases continuously on dilution of the vesicle dispersions from 100 to

Fig. 2 Second DSC upscan thermograms for 10–100 μM DODAB and DODAC in aqueous dispersions. The numbers besides the curves refer to DODAX concentration
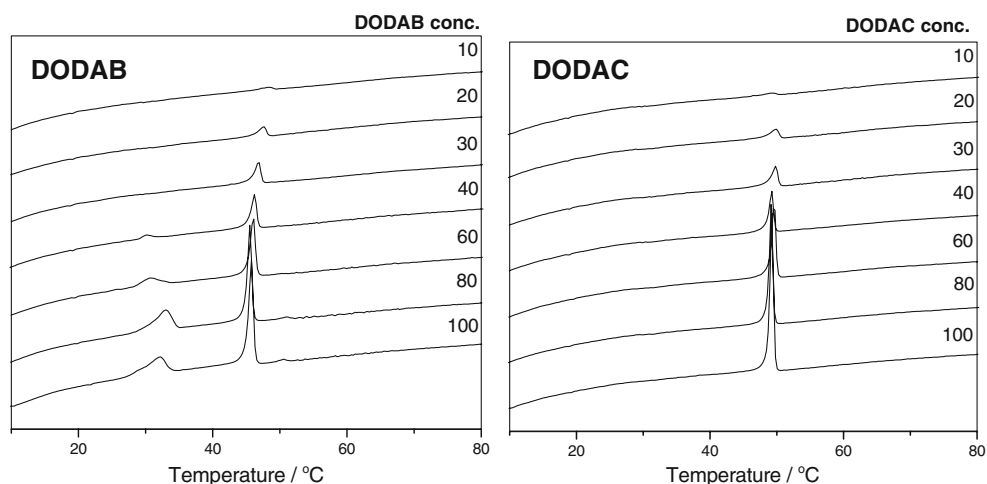
10 μM, with DODAB exhibiting a more pronounced increase (Fig. 3). Previously, it was reported that the T_m for DODAX in water increases when the vesicle size increases and planar bilayers (or bilayer fragments) exhibit even larger T_m [7]. In that communication [7], the vesicle size was controlled by extrusion while bilayer fragments were obtained by sonication. The data in Fig. 3 thus suggest that the micromolar DODAX aggregates may be slightly larger relative to the ordinary (1 mM) vesicles and/or that bilayer fragments are present. DODAB aggregates may exhibit higher change in size than DODAC ones. It is worth mentioning that DODAX vesicles were prepared spontaneously, that is, without sonication or extrusion that could influence the final aggregate structure or T_m. It was shown that at 1 mM concentration of DODAX, spontaneously prepared DODAB vesicles are larger than DODAC ones, despite the lower T_m for DODAB [11], which was attributed to the specificity of the counterion to the vesicles surface [11].

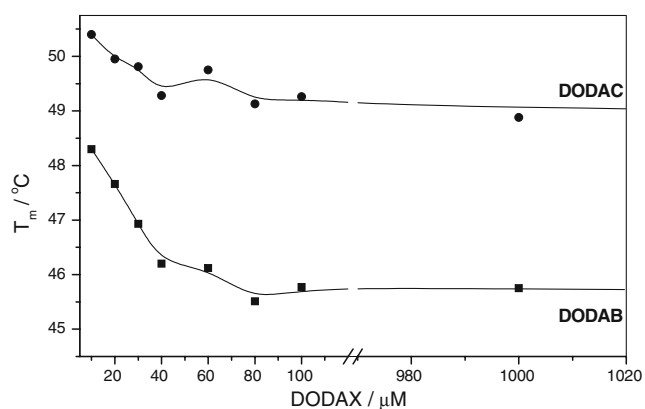Below ca 40 μM, T_m increases on sample dilution at a higher rate for DODAB. A linear fit of the first four points in the T_m curves (Fig. 3) gives $T_{m,0}=49.0$ and 50.7 °C, respectively for DODAB and DODAC at infinite dilution. The higher T_m for these aggregates relative to the ordinary vesicles could suggest the presence of bilayer fragments (planar structures), as reported [5, 12]. The precise structure of the micromolar aggregates requires further investigation.

The melting enthalpy increases as DODAX concentration is increased, with the enthalpy for DODAB being slightly smaller (Fig. 4), except at 20 μM. Overall, the melting enthalpy of DODAB is smaller than that for DODAC in agreement with the lower T_m of DODAB that requires smaller amount of heat to melt the surfactant chains. As the surfactant concentration increases, T_m decreases but ΔH increases, indicating the formation of more complex bilayer structures. One should realize that this is not a general behavior for lipid vesicles. An opposite behavior was reported for the anionic dihexadecylphos-
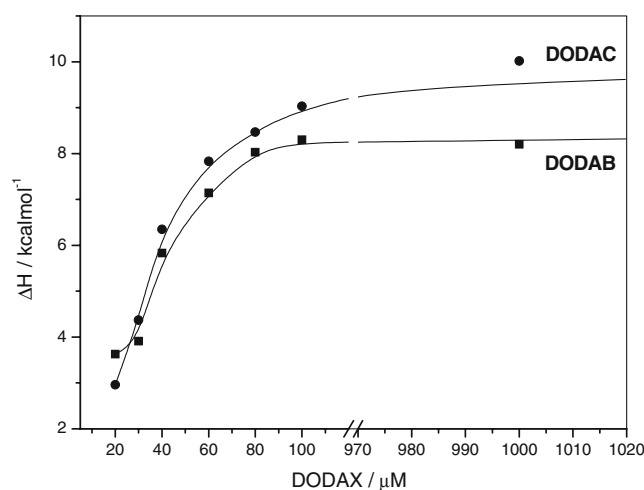

Fig. 3 The effect of surfactant concentration on the melting temperature, T_m, of DODAC and DODAB in water, obtained from the second DSC upscans. For comparison, the values of T_m for 1 mM were included

Fig. 4 The effect of surfactant concentration on the melting enthalpy, ΔH, of DODAC and DODAB in water, obtained from the second DSC upscans. For comparison, the values of ΔH for 1 mM DODAX were included

Table 1 Values of melting temperature (T_m), melting enthalpy (ΔH) and width of the melting transition peak ($\Delta T_{1/2}$) for different DODAB and DODAC molar concentrations

Conc./ μM	DODAB			DODAC		
	T_m/ °C	ΔH/kcal mol^{-1}	$\Delta T_{1/2}$/ °C	T_m/ °C	ΔH/kcal mol^{-1}	$\Delta T_{1/2}$/ °C
1,000	45.8	8.20	0.5	48.9	10.02	0.5
100	45.8	8.30	0.8	49.3	9.03	0.5
80	45.5	8.03	0.8	49.1	8.47	0.8
60	46.1	7.14	0.8	49.8	7.83	0.5
40	46.2	5.83	0.8	49.3	6.35	0.5
30	46.9	3.91	0.8	49.8	4.37	0.8
20	47.7	3.63	1.1	50.0	2.96	1.1

Data obtained from the second DSC upscans. Data for 10 μM not calculated because the peak is too small for data analyses

phate (DHP) vesicles in a HEPES buffer solution, for which both T_m and the melting enthalpy increase when DHP concentration is increased [13]. The width of the main transition peak, $\Delta T_{1/2}$, on the other hand, presents no clear dependence on surfactant concentration, but it lies between 0.5–1.0 (Table 1), characteristic of rather "sharp" cooperative transitions. The deviation in the $\Delta T_{1/2}$ data at the lowest DODAX concentrations may be due to the much smaller area of the peaks that leads to pronounced error in the calculation of this parameter.

Since the melting temperature is a characteristic of the surfactant bilayers, rather than the surfactant itself, in the domain of micromolar concentrations DODAX should assemble as bilayer structures, such as bilayer fragments due to larger T_m, as reported [5, 12]. The light-scattering

signal for the 10 μM DODAX dispersions is too weak, comparable to that for water (results not shown), thus, giving no information on the vesicle size.

Fluorescence results

NR has been extensively used as a fluorescence probe for microheterogeneous systems, such as vesicles, micelles and microemulsions, due to its hydrophobic nature [14–19]. In polar media, NR exhibits a solvatochromic behavior and displays a red shift of the emission maximum and fluorescence quenching, due to its capability to establish hydrogen bonds with protic solvents [20].

The hydrophobic nature of NR allows the probe to incorporate into the vesicle bilayer. The emission spectra of NR incorporated in the DODAX/water systems (Figs. 5 and 6) at 25 and 60°C, respectively, below and above the melting temperature of these surfactants, indicate a blue shift in the emission maximum with increasing surfactant concentration, relative to the spectrum in pure water. This indicates that as the surfactant concentration increases, the environment surrounding the probe is, in average, less hydrated, pointing to the presence of lipid aggregates. An increase in fluorescence intensity with DODAX concentration is also observed (inserts of Figs. 5 and 6), showing that at low surfactant concentrations the probe is more exposed to water.

For both DODAB and DODAC, the NR fluorescence exhibits a significant blue shift (lower λ_{max}) in the liquid-crystalline state (60°C), relative to the gel phase (25°C) (Fig. 7). Such a blue shift is not due only to the small thermochromic shift of the NR emission in pure water

Fig. 5 Normalized fluorescence spectra (λ_{exc}=550 nm) of 5×10^{-7}M NR in DODAB aqueous dispersions for several DODAB concentrations, at 25°C and 60°C, respectively, below and above T_m. Normalized emission of NR in pure water is shown for comparison. *Insert*: corresponding non-normalized emission spectra of NR in DODAB/water system
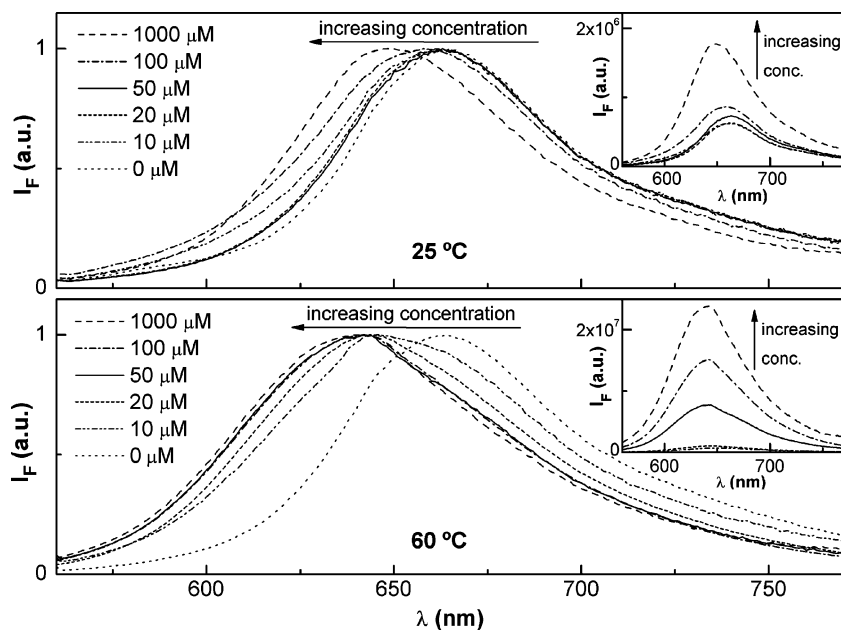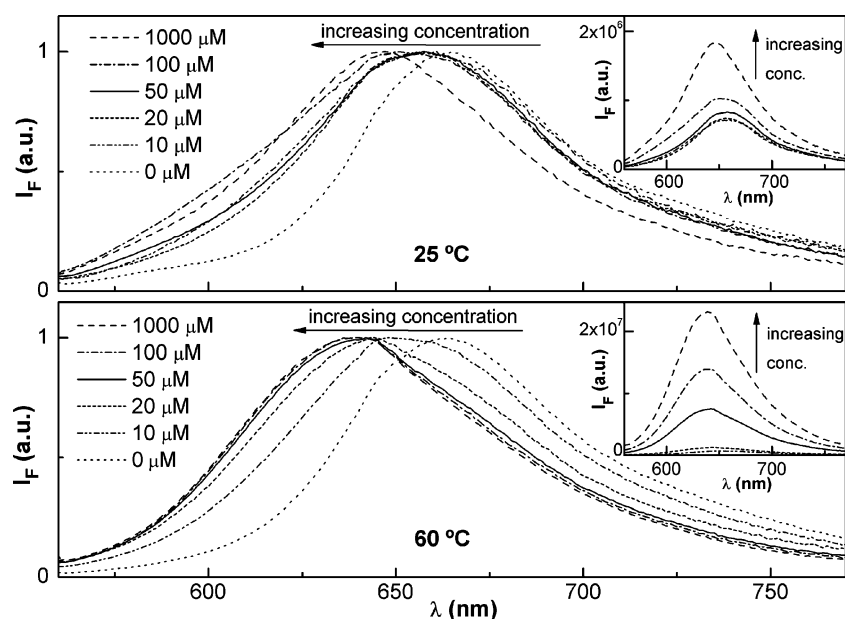
Fig. 6 Normalized fluorescence spectra (λ_{exc}=550 nm) of 5×10^{-7} M NR in DODAC aqueous dispersions for several DODAC concentrations, at 25°C and 60°C, respectively below and above T_m. Normalized emission of NR in pure water is shown for comparison. *Insert*: corresponding non-normalized emission spectra of NR in DODAC/water system

([DODAX]=0). It indicates that NR feels a more hydrophobic environment in the liquid-crystalline phase (above T_m), as previously observed for the DODAB/C_{18}TAB/water system [21]. At room temperature, the rigidity of the bilayers in the gel phase hinders the probe to penetrate deeper into the lipid bilayer. At 60°C, the lipid bilayers are in the liquid-crystalline state and DODAX concentration affects little λ_{max}, but the blue shift relative to pure water is much higher at 60 than at 25°C (Fig. 7).

For DODAC, the NR emission is always blue-shifted relative to DODAB (Fig. 7) and slightly more intense (insert of Figs. 5 and 6). This indicates that in DODAB aggregates, the NR environment is more hydrated, suggesting that DODAB bilayers are more densely packed than

DODAC bilayers, as previously reported [22], thus allowing the Br$^-$ to bind more tightly to the lipid interfaces than Cl$^-$ [7, 22, 23]. This prevents the fluorescent probe to penetrate deeper in the DODAB lipid aggregates.

Complementary information can be obtained from steady-state fluorescence anisotropy of NR in the DODAX/water systems. The anisotropy is given by

$$r = \frac{I_{VV} - G I_{VH}}{I_{VV} + 2 G I_{VH}} \quad (1)$$

where I_{VV} and I_{VH} are the intensity of the emission spectra obtained with vertical and horizontal light polarization, respectively, for vertically polarized excitation light, and

Fig. 7 Maximum emission wavelength of NR in DODAX/water systems, at 25°C and 60°C, for DODAB (*left*) and DODAC (*right*)
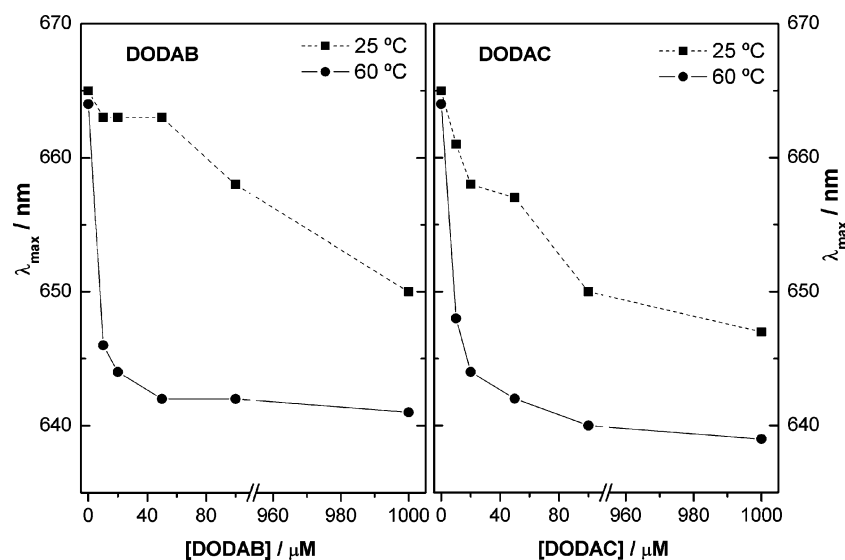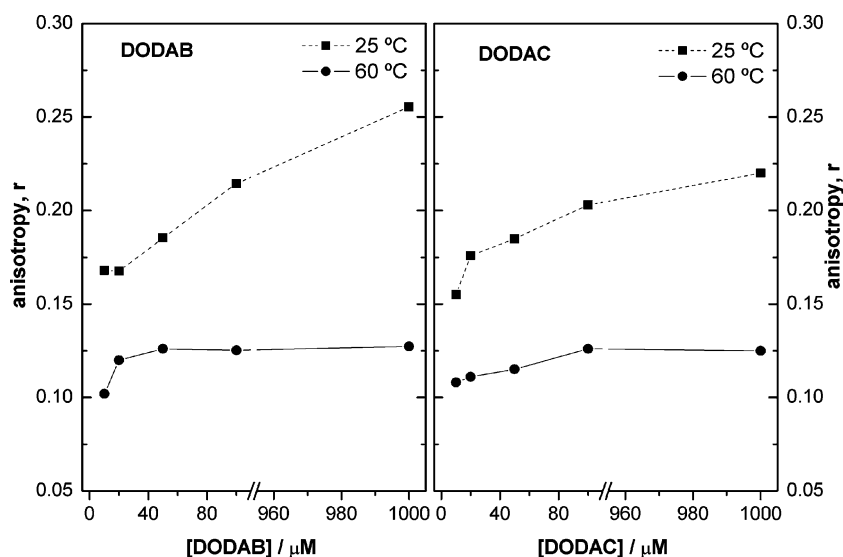
Fig. 8 Steady-state anisotropy of NR in DODAX/water systems, at 25°C and 60°C, for DODAB (*left*) and DODAC (*right*)

$G = I_{HV}/I_{HH}$ is the instrument correction factor, where I_{HV} and I_{HH} are the emission intensities obtained with vertical and horizontal light polarization, for horizontally polarized excitation light.

Since a high value of the anisotropy is related to a low degree of rotation of the probe, high anisotropy is expected when NR is located in a lipid bilayer, especially in the gel state (below T_m). On increasing temperature above T_m, a decrease in anisotropy is expected, resulting from the decrease in the bilayer microviscosity in the liquid-crystalline state.

At 1.0 mM DODAX and 25°C, the anisotropy is high, as reported for DODAB [19], because the vesicle bilayers of both surfactants are in the gel state (below T_m; Fig. 8). The

data suggest a lower fluidity of DODAB bilayer in the gel state of the ordinary vesicles relative to DODAC, consistent with a more dense packing of DODAB molecules relative to DODAC ones [22]. In the liquid-crystalline state, the fluidity of both DODAB and DODAC bilayers is rather similar to each other.

At 25°C, the anisotropy is generally high at all surfactant concentrations (Fig. 8), indicating that the rotation of the NR molecule is hindered in the DODAX/water systems, even at concentrations as low as 10 μM. Besides, the anisotropy exhibits a strong decrease by increasing temperature above T_m, reflecting the gel to liquid-crystalline state transition (melting) of the surfactant chains. This indicates

Fig. 9 Fitting of the NR emission spectrum in 10 μM DODAC at 25°C. The *dotted lines* correspond to the fitting components. **a** fitting to Eq. 2; **b** fitting to Eq. 3
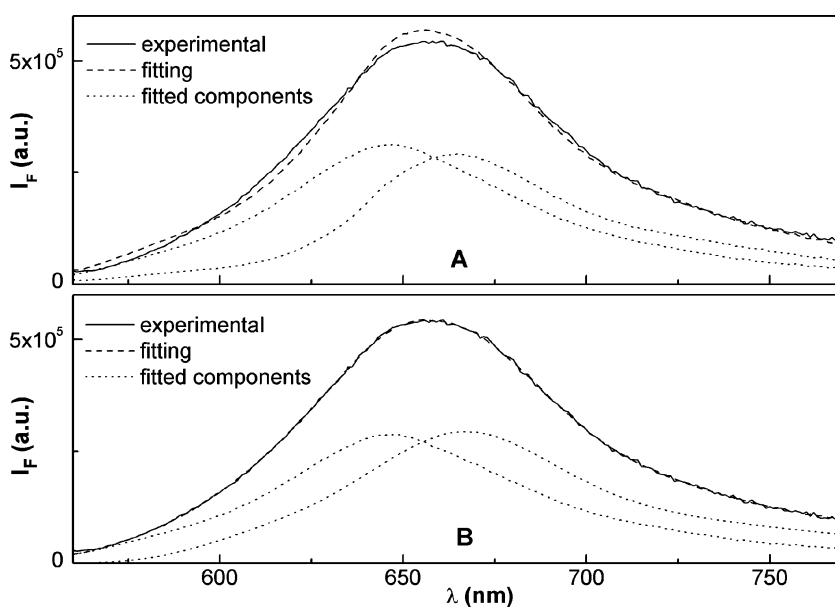
Table 2 Weights of the lognormal components obtained from the best fits to experimental NR emission in the DODAX/water systems at 25 °C (below T_m) and 60 °C (above T_m)

Conc/μM	DODAB				DODAC			
	25 °C($\lambda_{1\ mM}$=650 nm)		60 °C($\lambda_{1\ mM}$=641 nm)		25 °C($\lambda_{1\ mM}$=647 nm)		60 °C($\lambda_{1\ mM}$=639 nm)	
	λ_{fit}/nm	Weight	λ_{fit}/nm	Weight	λ_{fit}/nm	Weight	λ_{fit}/nm	Weight
100	662	61%	650	41%	660	29%	648	13%
50	662	64%	652	42%	662	43%	651	32%
20	663	65%	654	44%	663	48%	654	36%
10	663	71%	656	46%	663	51%	657	42%

The λ values correspond to maximum emission wavelengths

that even at micromolar concentrations, bilayer-like structures are present, in accordance with DSC results.

The decrease in anisotropy (especially for 10 and 20 μM DODAX, Fig. 8), together with the red shift and quenching of NR fluorescence at low DODAX concentrations, can be explained by the presence of a fraction of NR molecules located in a water-rich environment. As NR is a lipid probe, this more hydrated environment may correspond to the presence of planar bilayers or bilayer fragments, where NR molecules are more exposed to water and have a higher degree of rotation (lower r values). The monotonic increase of T_m on dilution of DODAX dispersions (Fig. 3), may also be explained by the presence of bilayer-like structures other than ordinary vesicles [7].

In fact, at low DODAX concentrations, the emission spectrum of NR seems to be composed by more than one single emission band. As the fluorescence band is asymmetric, the emission spectra can be decomposed into a sum of lognormal functions [24], an approach previously used for this probe in microheterogeneous systems [17, 25, 26]. Here, the NR spectra in the micromolar range of surfactant concentrations (10–100 μM) were first fitted as the sum of two components (Eq. 2), one corresponding to the NR experimental emission in 1.0 mM DODAX and the other to the NR emission in pure water, with variable fractions of each component, that is,

$$I_F = f_{1mM} I_{1mM} + f_{water} I_{water} \tag{2}$$

where I_F is the experimental emission spectrum, f_{1mM} is the fitted fraction of the NR emission in 1 mM DODAX (I_{1mM}) and f_{water} is the fitted fraction of NR emission in water (I_{water}). In almost all cases, the quality of these fittings is poor (an example is given in Fig. 9a).

Therefore, another approach was adopted, where one of the components is the NR emission in 1 mM DODAX (as before) and the other component, I_{fit}, is a lognormal function (or the sum of two lognormal functions, if

necessary) obtained from the best fit to the experimental results (Eq. 3).

$$I_F = f_{1mM} I_{1mM} + I_{fit} \tag{3}$$

with

$$I_{fit} = \frac{A}{(\lambda - \lambda_{max} + a)} \exp(-c^2)$$
$$\times \exp\left\{ -\frac{1}{2c^2} \left[\ln\left(\frac{\lambda - \lambda_{max} + a}{b} \right) \right]^2 \right\}, \tag{4}$$

where A is the maximum emission intensity at wavelength λ_{max} and the parameters a, b, and c are given by [24]

$$c = \ln(\rho) \Big/ \sqrt{2\ln(2)} \qquad b = H \frac{\rho}{\rho^2 - 1} \exp(c^2) \tag{5}$$
$$a = H \frac{\rho}{\rho^2 - 1}$$

where H is the half-width of the band and ρ is the skewness.

For both surfactants at 25 °C, the experimental emission is well described by a fitted fraction of NR emission in 1 mM DODAX and one lognormal function with λ_{max} around 660−663 nm (Fig. 9b), which is characteristic for the probe in a water-rich environment (NR maximum emission wavelength in water at 25 °C is 665 nm). The weight of the latter component increases with the decrease in surfactant concentration (Table 2). This can explain the decrease in the NR anisotropy at low DODAX concentrations, as this water-rich medium can correspond to a less viscous environment. The weight of this component is always higher for DODAB than for DODAC. The slightly lower NR anisotropy for DODAC at room temperature (Fig. 8) points to a more fluid (less compact) bilayer than DODAB, as reported in a previous work [22], allowing a

higher fraction of probe molecules to penetrate deep into the DODAC bilayer.

The results at 60 °C confirm that in the liquid-crystalline state the NR molecules can penetrate deeper into the DODAX bilayers, and the fitted lognormal component corresponding to a more hydrated environment has a lower weight (Table 2). At this high temperature, the majority of the NR molecules feel an environment close to the one in ordinary (1 mM DODAX) vesicles. The other fraction of molecules (component with λ_{max}=648−657 nm) is more significant in DODAB than in DODAC micromolar bilayers. Results of DSC and NR fluorescence can be explained by a higher number of bilayer fragments or planar bilayers in DODAB/water system, where a stronger influence of surfactant concentration can be observed in both T_m and anisotropy values.

Summary

The DSC and Nile Red fluorescence data here reported indicate that bilayer-like aggregates of DODAX (X representing Br$^-$ or Cl$^-$) in water are formed in the micromolar domain of the surfactant concentration, that is, at concentrations as low as 10 μM.

In theory, these aggregates are formed above DODAX CVC. The physical characterization of these structures is quite difficult to be determined, because a limited amount of sensitive enough techniques, such as DSC and fluorescence, is available to investigate such diluted systems. They cannot be viewed, for instance, by cryogenic transmission electron microscopy (cryo-TEM) or detected by scattering techniques.

An important characteristic of DODAX to be appropriate to form bilayer-like aggregates is that their CVC is very low (3.7×10^{-9} M for DODAB) [5], thus, allowing the formation of bilayer structures at concentrations as low as 10 μM.

Since T_m is a characteristic of surfactant bilayers, and since in the millimolar concentration domain (e.g., 1 mM) DODAX vesicles exhibit mainly the melting temperature transition, the DSC peak detected for DODAX dispersions in the micromolar concentration domain is clearly due to bilayer-like aggregates. The investigation of the precise structure of such aggregates is underway by our group.

Like the ordinary vesicles, DODAX micromolar-bilayer-like aggregates have potential applications as vehicles for drug delivery since they solubilize small molecules, such as the NR probe here investigated.

References

1. Lasic DD (1993) Liposomes. From physics to applications. Elsevier, Amsterdam
2. Fendler JH (1982) Membrane mimetic chemistry. Wiley, New York
3. Carmona-Ribeiro AM (1992) Synthetic amphiphile vesicles. Chem Soc Rev 21:209
4. Cuccovia IM, Sesso A, Abuin EB, Okino PF, Tavares PG, Campos JFS, Florenzano FH, Chaimovich H (1997) J Mol Liq 72:323
5. Feitosa E, Brown W (1997) Langmuir 13:4810
6. Blandamer MJ, Briggs B, Cullis PM, Last P, Engberts JBFN, Kacperska A (1999) J Therm Anal Calorim 55:29
7. Feitosa E, Barreleiro PCA, Olofsson G (2000) Chem Phys Lipids 105:201
8. Benatti CR, Feitosa E, Fernandez RM, Lamy-Freund MT (2001) Chem Phys Lipids 111:93
9. Feitosa E, Barreleiro PCA (2004) Prog Coll Polym Sci 128:163
10. Brito RO, Marques EF (2005) Chem Phys Lipids 137:18
11. Feitosa E, Karlsson G, Edwards K (2006) Chem Phys Lipids 140:66
12. Feitosa E, Alves FR (2008) Chem Phys Lipids 156:13
13. Feitosa E (2008) J Colloid Interface Sci 320:608
14. Greenspan P, Mayer EP, Fowler SD (1985) J Cell Biol 100:965
15. Greenspan P, Fowler SD (1985) J Lipid Res 26:781
16. Krishnamoorthy IG (2001) J Phys Chem B 15:1484
17. Hungerford G, Castanheira EMS, Real Oliveira MECD, Miguel MG, Burrows HD (2002) Phys Chem B 106:4061
18. Hungerford G, Castanheira EMS, Baptista ALF, Coutinho PJG, Real Oliveira MECD (2005) J Fluorescence 15:835
19. Feitosa E, Alves FR, Niemiec A, Real Oliveira MECD, Castanheira EMS, Baptista ALF (2006) Langmuir 22:3579
20. Cser A, Nagy K, Biczók L (2002) Chem Phys Lett 360:473
21. Alves FR, Zaniquelli MED, Loh W, Castanheira EMS, Real Oliveira MECD, Feitosa E (2007) J Colloid Interface Sci 316:132
22. Lopes A, Edwards K, Feitosa E (2008) J Colloid Interface Sci 322:582
23. Nascimento DB, Rapuano R, Lessa MM, Carmona-Ribeiro AM (1998) Langmuir 14:7387
24. Siano DB, Metzler DE (1969) J Chem Phys 51:1856
25. Srivatsavoy VJP (1999) J Lumines 82:17
26. Coutinho PJG, Castanheira EMS, Rei MC, Real Oliveira MECD (2002) J Phys Chem B 106:2841